

Atomic and entanglement dynamics in the mixed squeezed coherent state version of the Jaynes-Cummings interaction

Koushik Mandal*

Department of Physics, Indian Institute of Technology Madras, Chennai 600036, India

Pooja Jethwani†

School of Physical Sciences, National Institute of Science Education and Research, Bhubaneswar, HBNI, Jatni, Odisha-752050, India

M. Venkata Satyanarayana‡

Department of Physics, Indian Institute of Technology Madras, Chennai 600036, India.

Abstract. The main objective of this work is to study the mixed state version of the Jaynes-Cummings model in the context of two-level atom interacting with a mixed field state of a squeezed vacuum and a coherent state. Here, the pure squeezed coherent state (PSCS) and the mixed squeezed coherent state (MSCS) have been used as the states of the radiation field. The photon-counting distribution (PCD), the atomic inversion and the entanglement dynamics of atom-field interaction for both the radiation fields are investigated and compared with each other. We observe that depending on the state of the field, squeezing has very different effects on coherent photons. Mild squeezing on the coherent photons localizes the PCD for PSCS; however, for MSCS there is no such localization observed - instead squeezing manifests for MSCS as oscillations in the PCD. The effects of squeezing on the atomic inversion and the entanglement dynamics for PSCS are very different as compared with the corresponding quantities associated with MSCS; in fact, they are contrasting. It is well known in the literature that for PSCS, increasing the squeezing increases the well-known ringing revivals in the atomic inversion, and also increases irregularity in the entanglement dynamics. However, increasing the squeezing in MSCS very significantly alters the collapse-revival pattern in the atomic inversion and the entanglement dynamics of the Jaynes-Cummings model. For MSCS, the effect of squeezing on the quadrature variables and Mandel's Q parameter are also presented.

I. INTRODUCTION

The study of interactions between atom and field is one of the major topics in quantum optics. The quantities like the photon counting distribution, the atomic inversion, and the entanglement dynamics have been at the centre of interest in quantum optics. Also, entanglement is an important aspect of quantum information, quantum cryptography, and quantum computation. The interaction between the radiation field and the two-level atoms provides a way to study the entanglement dynamics between the two systems.

In literature, to investigate the atom-radiation interaction, various models have been used, depending on the nature of interaction, like type and strength, etc. In the present study, we have used the Jaynes-Cummings model (J-C model), which is a paradigm model of interaction in quantum optics [1, 2]. Using this model, Subeesh *et al.*, have studied the dynamics of atom-field interaction, where they took the radiation field to be in a pure squeezed coherent

state (PSCS) and the atom as a two-level system, and they have studied the photon counting distribution (PCD), the atomic inversion ($W(t)$) and the entanglement dynamics [3]. They observed that the addition of squeezed photons has a drastic effect on the PCD. Even an addition of 2% of squeezed photons can localize the PCD very significantly to 100%. They also observed that on further increasing the squeezing, the PCD reaches a maximum and then on decreases with build up in tailing oscillations. This oscillatory behaviour of the PCD explains the ringing revivals effect in the atomic inversion [4]. It also affects the entanglement dynamics [3]. Earlier, Satyanarayana *et al.*, have used the J-C model to study the atom-field interaction, where the field is in a superposition of thermal and coherent states [4]. This superposition is called as the Glauber-Lachs mixing. They showed that the addition of thermal photons drastically alters both the PCD and the atomic inversion: the addition of even one thermal photon on average to 50 mean coherent photons the PCD leads to a 50% decline in the PCD peak. So, the addition of thermal photons to a coherent state delocalises the PCD. They also observed that the atomic inversion has a rather drastic response to the addition of thermal photons.

Sivakumar compared the Glauber-Lachs super-

* ph17d030@smail.iitm.ac.in

† pooja.jethwani@niser.ac.in

‡ mvs@iitm.ac.in

position with the mixed thermal coherent state (MTCS) at the level of density operator [5]. The atomic inversion and the entanglement dynamics of both the states were compared, and it was reported that the MTCS is more sensitive to the thermal photon addition as opposed to the thermal photon addition in the G-L mixing.

In the recent years, various studies have been carried out on the squeezed coherent states i.e., here the PSCS. Geore Moulouden and Peter Conbropoulos have studied the Squeezed coherent states in double optical resonance [6]; Zhen Way *et al.*, have investigated the statistical properties of photon-added two mode squeezed coherent states [7]. Studies have been done to create entangled coherent states by mixing squeezed vacuum and coherent light [8] and to find the time-evolution of squeezed coherent states of a generalized quantum parametric oscillator [9]. Also in quantum information and computation, the squeezed coherent states have been used [10, 11].

In this work, the field is taken to be in a mixed squeezed coherent state (MSCS), which has not been studied so far. The coherent photons are treated as signal and the squeezed photons as noise. In this work, the PCD, the atomic inversion and the entanglement dynamics for MSCS have been evaluated and these properties have been compared with those of the PSCS. Such a study is interesting as the results are quite contrary to those corresponding to the PSCS.

The organisation of this paper is as follows: in Section II, the MSCS is defined and the corresponding PCD is obtained. In Section III, the Jaynes-Cummings interaction of MSCS is studied. The focus is to bring out the differences in the evolution of the population inversion and the evolution of entanglement when the atom interacts with the PSCS and MSCS. In the following sections, the quadrature squeezing, Mandel's Q parameter and the Wigner function of MSCS are also presented.

II. PHOTON COUNTING DISTRIBUTION (PCD)

The squeezed coherent states are defined as

$$|\alpha, \zeta\rangle \equiv \hat{D}(\alpha)\hat{S}(\zeta)|0\rangle. \quad (1)$$

Now, the density matrices for pure squeezed coherent states (PSCS) and mixed squeezed coherent states (MSCS) are given by,

$$\hat{\rho}_{\text{pure}} = |\alpha, \zeta\rangle \langle \alpha, \zeta|, \quad (2)$$

and

$$\hat{\rho}_{\text{mixed}} = q |\alpha\rangle \langle \alpha| + (1 - q) |\zeta\rangle \langle \zeta|, \quad (3)$$

where q is the probability of the field to be in the coherent state and $(1 - q)$ is the probability to be in the squeezed state. In this study, the field is prepared in the MSCS as in Eq. (3) and various quantum optical quantities associated with these states are compared with the corresponding quantities of the PSCS.

To study the interaction dynamics of the atom with two different states of fields, we need to fix a parameter which is common to both the fields. Here, for PSCS and MSCS, average number of coherent photons N_c and average number of squeezed photons N_s are common, but q which occurs only in MSCS is a variable. It is essential to fix the value of q so that the states have same mean number of photons. But, for PSCS $\langle n \rangle = N_c + N_s$ and for MSCS $\langle n \rangle = qN_c + (1 - q)N_s$. So, by equating the mean number of photons we will never get a solution for q . Another way to choose the value of q is by equating the overlap with the coherent state for both the PSCS and MSCS, i.e., $\langle \alpha | \hat{\rho}_{\text{pure}} | \alpha \rangle = \langle \alpha | \hat{\rho}_{\text{mixed}} | \alpha \rangle$. The contributions of coherent state to PSCS and MSCS are given by the following equations respectively;

$$\langle \alpha | \hat{\rho}_{\text{pure}} | \alpha \rangle = \text{sech} |\zeta|, \quad (4)$$

$$\begin{aligned} \langle \alpha | \hat{\rho}_{\text{mixed}} | \alpha \rangle &= q + (1 - q) \text{sech} |\zeta| \\ &\times \exp \left[-2 \left(\frac{\alpha_R^2}{\exp(-2|\zeta|) + 1} + \frac{\alpha_I^2}{\exp(2|\zeta|) + 1} \right) \right], \end{aligned} \quad (5)$$

where α_R and α_I are the real and imaginary parts of α respectively. Solving these equations for real part of α we get

$$q = \frac{\text{sech} |\zeta| [1 - \exp(-\alpha_R^2(1 + \tanh |\zeta|))]}{1 - \text{sech} |\zeta| \exp(-\alpha_R^2(1 + \tanh |\zeta|))}. \quad (6)$$

From eqn.6 we observe that if $|\zeta| = 0$, q becomes 1. So now both PSCS and MSCS are pure coherent state. But, if $\alpha = 0$ then $q = 0$. In this case both the states become pure squeezed states. So, the equal overlap of the coherent state implies that the limiting cases of PSCS and MSCS are the same.

The PCD for the PSCS is given by [3, 12, 13],

$$\begin{aligned} P(n) &= \frac{1}{n! \mu} \left(\frac{\nu}{2\mu} \right)^2 H_n^2 \left(\frac{\beta}{\sqrt{2\mu\nu}} \right) \\ &\times \exp \left(-\beta^2 \left(1 - \frac{\nu}{\mu} \right) \right), \end{aligned} \quad (7)$$

where $\mu = \cosh|\zeta| = \sqrt{1+N_s}$, $\nu = \sinh|\zeta| = \sqrt{N_s}$ and $\beta = \sqrt{N_c}(\sqrt{1+N_s} + \sqrt{N_s})$; N_s = average number of squeezed photons and N_c = average number of coherent photons.

The PCD for the MSCS is given by [14],

$$P(n) = q|\langle n|\alpha\rangle|^2 + (1-q)|\langle n|\zeta\rangle|^2, \quad (8)$$

$$P(n) = \begin{cases} q \exp(-N_c) \frac{N_c^n}{n!} + \frac{(1-q)}{\sqrt{1+N_s}} \frac{n!}{2^n (\frac{n}{2}!)^2} \\ \times \left(\sqrt{\frac{N_s}{1+N_s}} \right)^n, & \text{for } n \text{ is even} \\ q \exp(-N_c) \frac{N_c^n}{n!}, & \text{for } n \text{ is odd.} \end{cases} \quad (9)$$

The average number of photons in MSCS is given by

$$\bar{n}_{avg} = qN_c + (1-q)N_s. \quad (10)$$

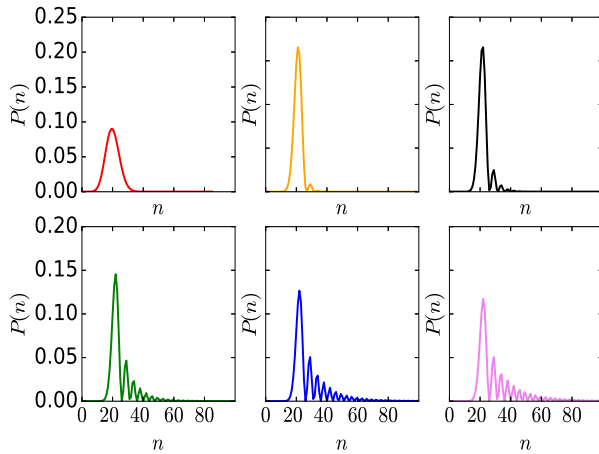


FIG. 1: Photon counting distribution of PSCS for $N_c = 20$, $N_s = 0, 1, 2, 5, 8, 10$.

In Fig. 1 we have plotted the PCD for PSCS for $N_c = 20$; $N_s = 0, 1, 2, 5, 8, 10$. We observe from the plots that for $N_s = 0$, it is just the PCD of a coherent state with $N_c = 20$. Now, as we increase the squeezed photons, the PCD changes significantly. For $N_s = 1$, the peak of the PCD becomes almost double the peak for $N_s = 0$, i.e., the PCD gets localized. Also, we see that the PCD begins to oscillate [15]. If we increase N_s further, the peak of the PCD comes down and the oscillatory behaviour becomes very significant. This oscillatory behaviour of the PCD is manifested in the atomic inversion and in the entanglement dynamics [3].

Fig. 2 represents the PCD for MSCS. For the MSCS, initially we have taken $N_c = 20$ and $N_s = 0$. For $N_s = 0$, the PCD is that of a coherent state.

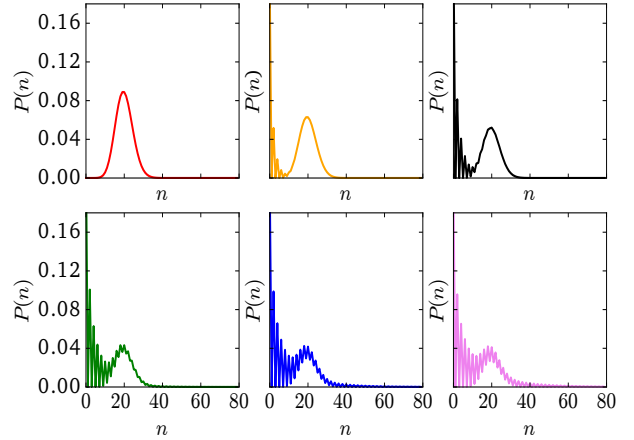


FIG. 2: Photon counting distribution of MSCS for $N_c = 20$, $N_s = 0, 1, 2, 5, 8, 10$ and $q = 1.00, 0.70, 0.58, 0.41, 0.33, 0.30$

Now, if we increase the value of N_s , say $N_s = 1, 2$, we see oscillations start at the beginning, but there are no oscillations at the tail of the PCD. If we increase N_s further, say $N_s = 5$, the oscillatory behaviour - though not very pronounced - is seen till the tail of the PCD. Addition of squeezed photons do not destroy the signature peak of the coherent state PCD. Instead, they introduce high frequency oscillations enveloping the peak representing coherent state. On increasing the number of squeezed photons, the enveloping oscillations become more pronounced with a gradual decrease in the coherent state peak. The oscillations at the tail increases with N_s . This oscillatory behaviour comes due to the PCD of squeezed states.

The main contrast in the behaviour of the PCD of MSCS is that with the increase in squeezing, it set about with oscillations for small values of n . This behaviours to be compared with the tail of PCD of PSCS, which picks up oscillations, with the increase in squeezing. So, a very small amount of squeezing is dominant to bring in the oscillations in the PCD of MSCS, the tail picks up oscillations as in the case of PSCS. Another important fact that differentiates between the PCD of PSCS and the PCD of MSCS is that there is no localization of the PCD in the case of MSCS.

III. DENSITY MATRIX APPROACH TO THE ATOM-FIELD INTERACTION

The Jaynes-Cummings interaction Hamiltonian for the atom-field interaction is well studied in quantum optics and it is given by [1]

$$\hat{H} = \hbar\omega\hat{a}^\dagger\hat{a} + \frac{\hbar\omega_0}{2}\hat{\sigma}_z + \hbar\lambda(\hat{\sigma}_+\hat{a} + \hat{\sigma}_-\hat{a}^\dagger), \quad (11)$$

where $\hat{\sigma}_+$, $\hat{\sigma}_-$ and $\hat{\sigma}_z$ are the Pauli pseudospin operators; \hat{a} and \hat{a}^\dagger are the photon annihilation and the photon creation operators; λ is the coupling constant describing the atom-field interaction; ω is the field frequency and ω_0 is the atomic transition frequency.

Under the interaction picture, if we use the resonant condition, i.e., the detuning $\Delta = \omega - \omega_0 = 0$, the interaction Hamiltonian becomes

$$\hat{H}_I = \hbar\lambda(\hat{\sigma}_+\hat{a} + \hat{\sigma}_-\hat{a}^\dagger). \quad (12)$$

Let $|g\rangle$, $|e\rangle$ are the ground state and the excited state of the atom respectively and $|n\rangle$ are the Fock states of the radiation field. The action of \hat{H}_I on the total initial state $|e, n\rangle$ of the atom-field system assuming that the atom initially in the excited state is given by the following equations,

$$\hat{H}_I |e, n\rangle = \hbar\lambda\sqrt{n+1} |g, n+1\rangle, \quad (13)$$

$$\hat{H}_I |g, n+1\rangle = \hbar\lambda\sqrt{n} |e, n\rangle. \quad (14)$$

We define $\hat{\rho}_{\text{tot}}(t)$ to be the total density operator of the atom-field system at time t , and the time evolution of this operator can be written as,

$$\hat{\rho}_{\text{tot}}(t) = \hat{U}(t)\hat{\rho}_{\text{tot}}(0)\hat{U}^\dagger(t), \quad (15)$$

where $\hat{U}(t) = \exp(-i\frac{\hat{H}_I t}{\hbar})$ is the unitary time evolution operator.

$\hat{U}(t)$ can be expanded in the two dimensional subspace as [16]

$$\hat{U}(t) = \begin{pmatrix} \hat{C}(t) & \hat{S}'(t) \\ \hat{S}(t) & \hat{C}'(t) \end{pmatrix}, \quad (16)$$

where

$$\hat{C}(t) = \cos(\lambda t\sqrt{\hat{a}\hat{a}^\dagger}), \quad (17)$$

$$\hat{S}(t) = -i\frac{\hat{a}^\dagger \sin(\lambda t\sqrt{\hat{a}\hat{a}^\dagger})}{\sqrt{\hat{a}\hat{a}^\dagger}}, \quad (18)$$

$$\hat{C}'(t) = \cos(\lambda t\sqrt{\hat{a}^\dagger\hat{a}}), \quad (19)$$

$$\hat{S}'(t) = -i\frac{\hat{a} \sin(\lambda t\sqrt{\hat{a}^\dagger\hat{a}})}{\sqrt{\hat{a}^\dagger\hat{a}}}. \quad (20)$$

$$(21)$$

Now, if $\hat{\rho}_F(0)$ is the density matrix for the field and $\hat{\rho}_{\text{atom}}$ is the density operator of the atom, then

the initial density operator for the atom-field system is given by,

$$\hat{\rho}_{\text{tot}}(0) = \hat{\rho}_F(0) \otimes \hat{\rho}_{\text{atom}}. \quad (22)$$

Initially, this atom-field system may be unentangled; but during the time evolution the system may get entangled, which is a characteristic feature of the bipartite nature of the system.

We assume that the atom is initially in the excited state $|e\rangle$, so $\hat{\rho}_{\text{atom}}(0) = |e\rangle\langle e|$. In matrix form

$$\hat{\rho}_{\text{atom}}(0) = \begin{pmatrix} 1 & 0 \\ 0 & 0 \end{pmatrix}. \quad (23)$$

Under the time evolution $\hat{\rho}_{\text{tot}}(t)$ becomes [5, 16]

$$\hat{\rho}_{\text{tot}}(t) = \begin{pmatrix} \hat{C}(t)\hat{\rho}_F(0)\hat{C}'(t) & -\hat{C}(t)\hat{\rho}_F(0)\hat{S}'(t) \\ \hat{S}(t)\hat{\rho}_F(0)\hat{C}(t) & -\hat{S}(t)\hat{\rho}_F(0)\hat{S}(t) \end{pmatrix}. \quad (24)$$

IV. ATOMIC INVERSION

To calculate the atomic inversion $W(t)$, first we need to find the atomic density matrix $\hat{\rho}_{\text{atom}}$ from $\hat{\rho}_{\text{tot}}(t)$. This is done by tracing over the density matrix over the field state. So,

$$\hat{\rho}_{\text{atom}}(t) = \text{Tr}_{\text{field}}[\hat{\rho}_{\text{tot}}(t)] \quad (25)$$

$$= \sum_{n=0}^{\infty} \langle n | \hat{\rho}_{\text{tot}}(t) | n \rangle. \quad (26)$$

The atomic inversion, which is defined as the difference in the probabilities of finding the atom in the excited state and ground state, is given as [16]

$$W(t) = \langle \hat{\sigma}_3 \rangle \quad (27)$$

$$= \text{Tr}[\hat{\rho}_{\text{atom}}(t)\hat{\sigma}_3] \quad (28)$$

$$= \sum_{n=0}^{\infty} \langle n | \hat{\rho}_F(0) | n \rangle \cos(2\lambda\sqrt{n+1} t) \quad (29)$$

$$= \sum_{n=0}^{\infty} P(n) \cos(2\lambda\sqrt{n+1} t). \quad (30)$$

So, the $W(t)$ for the PSCS is given by

$$W(t) = \sum_{n=0}^{\infty} \langle n | \alpha, \zeta \rangle \langle \alpha, \zeta | n \rangle \cos(2\lambda\sqrt{n+1} t), \quad (31)$$

where $|\langle n | \alpha, \zeta \rangle|^2$ is the PCD for PSCS given by Eq.(7). For the MSCS, the atomic inversion $W(t)$ is given by

$$W(t) = \sum_{n=0}^{\infty} \left[\left\{ q \exp(-N_c) \frac{N_c^{2n}}{(2n)!} + \frac{(1-q)}{\sqrt{1+N_s}} \frac{(2n)!}{2^{2n}(n!)^2} \left(\frac{N_s}{1+N_s} \right)^n \right\} \cos(2\lambda t \sqrt{2n+1}) + \left\{ q \exp(-N_c) \frac{N_c^{2n+1}}{(2n+1)!} \right\} \cos(2\lambda t \sqrt{2n+2}) \right], \quad (32)$$

where N_c is the average number of coherent photons and N_s is average number of squeezed photons.

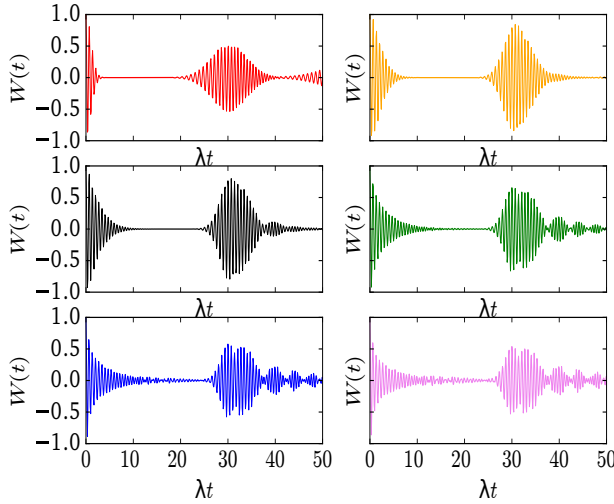


FIG. 3: Atomic inversion $W(t)$ vs λt for PSCS for $N_c = 20$, $N_s = 0, 1, 2, 5, 8, 10$.

The temporal variations of atomic inversion for both the PSCS and the MSCS are shown in Figs. 3 and 4 respectively. We have plotted $W(t)$ vs λt , where λt is the scaled time.

To investigate the atomic inversion for both the states MSCS and PSCS, we have taken the average number of coherent photons $N_c = 20$ and the squeezed photons $N_s = 0, 1, 2, 5, 8, 10$. We observe that $W(t)$ for both the states starts from that of a coherent state; but addition of squeezing to the fields has very different behaviour compared to each other. If we add a single squeezed photon to the PSCS, we observe that the collapse time of $W(t)$ becomes small and oscillatory. On further increasing the value of squeezing, the collapse time gets smaller with ringing revivals on its dynamics.

In the case of MSCS, $W(t)$ behaves differently. If we add a single squeezed photon, the collapse phenomena gets destroyed completely. If we increase the squeezing further, the pattern remains almost same with no ringing revivals in its dynamics as we observed in the case of PSCS. From the behaviours

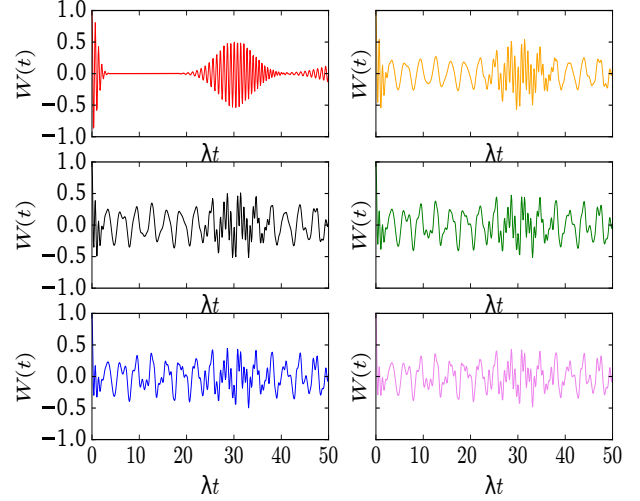


FIG. 4: Atomic inversion $W(t)$ vs λt for MSCS for $N_c = 20$, $N_s = 0, 1, 2, 5, 8, 10$ and $q = 1.00, 0.70, 0.58, 0.41, 0.33, 0.30$.

of $W(t)$ for both the states, it can be concluded that the addition of squeezing has more sensitive effects on the atomic dynamics for MSCS as compared to the case of PSCS.

V. ENTANGLEMENT DYNAMICS

There are various quantities that measure the entanglement between two systems, like, von Neumann entropy and linear entropy, etc. Here, for a mixed state, to measure the entanglement between the atom and the field, the logarithmic negativity $N(t)$ has been used, which is defined as the absolute sum of the negative eigenvalues of the partially transposed density operator $\hat{\rho}_{\text{tot}}^{PT}$ [17, 18]. If, λ_k are the eigenvalues of $\hat{\rho}_{\text{tot}}^{PT}$, then $N(t)$ is given by

$$N(t) = \sum_k [|\lambda_k| - \lambda_k] / 2. \quad (33)$$

Figs. 5 and 6 represent the entanglement dynamics for the PSCS and the MSCS respectively.

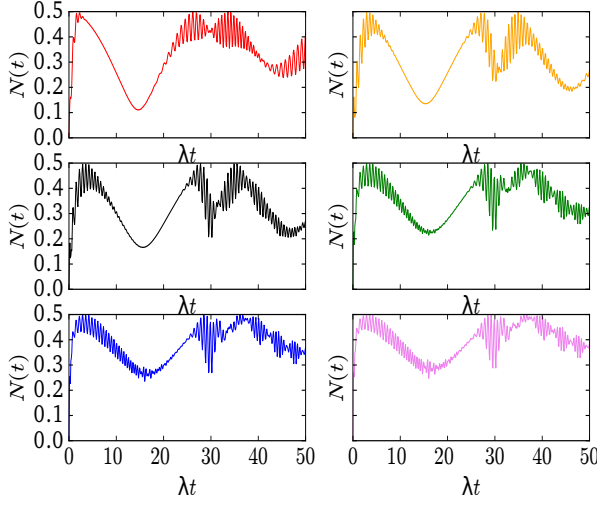


FIG. 5: Entanglement dynamics $N(t)$ vs λt for PSCS for $N_c = 20$, $N_s = 0, 1, 2, 5, 8, 10$.

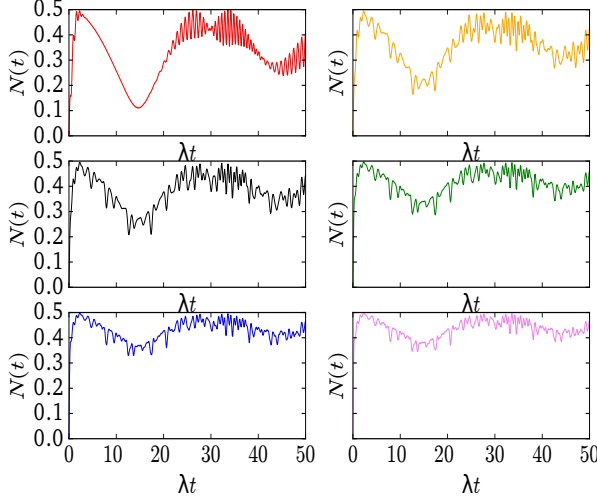


FIG. 6: Entanglement dynamics $N(t)$ vs λt for MSCS for $N_c = 20$, $N_s = 0, 1, 2, 5, 8, 10$ and $q = 1.00, 0.70, 0.58, 0.41, 0.33, 0.30$.

Like the atomic inversion, here also we have taken the average number of coherent photons $N_c = 20$, the squeezed photons $N_s = 0, 1, 2, 5, 8, 10$ and $q = 1.00, 0.70, 0.58, 0.41, 0.33, 0.30$. For the PSCS, $N(t)$ starts from the coherent state dynamics as like $W(t)$. On addition of squeezed photons in the field, slight oscillations build up in the smooth collapse part of the dynamics and the second collapse point comes down significantly. With the further increase in the squeezing, the minimum value of the first collapse of $N(t)$ gets higher and the oscillations in the collapse

part become more prominent. This pattern continues for other higher values of N_s .

For the MSCS, $N(t)$ starts from the coherent state dynamics also. Here, if we add a squeezed photon, all the collapse parts become oscillatory and the minimum value of $N(t)$ gets higher. On further increasing the squeezing, the amplitude of the oscillations in the dynamics becomes smaller and the minimum values become higher. One interesting fact is that the amplitude of the oscillation of $N(t)$ for MSCS becomes smaller with increasing squeezing but for PSCS, the amplitude of oscillations in the dynamics of $N(t)$ becomes larger. Since, $N(t)$ represents the extent of entanglement of the atom with the radiation field, it is observed that as the squeezing is increased, this entanglement gets stronger even during the collapse part. This effect is significantly enhanced in MSCS as compared to PSCS.

VI. ATOMIC INVERSION AND ENTANGLEMENT DYNAMICS FOR A FIXED VALUE OF WEIGHTAGE PARAMETER(q)

In the last two sections we have studied the atomic-inversion and the entanglement dynamics for different values of q which is dependent on N_c and N_s . In this section we want to investigate the effects of fixed value of q on the atom-field interaction dynamics. We have taken $q = 0.8$, i.e., 80% of the field is coherent which is justified if we consider the coherent states as the signal and squeezed states as noise.

A. Photon Counting Distribution

The PCDs for PSCS and MSCS are plotted in the Figs. 7 and 8. For these plots we have taken $N_c = 10$, $N_s = 0, 1, 2, 5, 8, 10$ and $q = 0.8$. We observe that the PCD for PSCS for $N_c = 10$ mimics the pattern for $N_c = 20$; but for MSCS, the oscillations in the very small compared to the PCD for $N_c = 20$. For MSCS, the PCD remains almost like a coherent state with little oscillations at the beginning and the tail of the PCD.

B. Atomic Inversion

In order to calculate the atomic inversion for MSCS and PSCS, we have taken the average number of coherent photons $N_c = 10$ and the squeezed photons $N_s = 0, 1, 2, 5, 8, 10$.

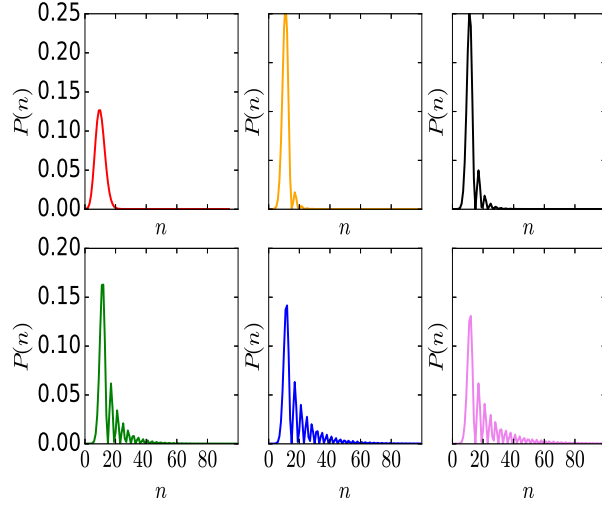


FIG. 7: $P(n)$ vs n for PSCS for $N_c = 10$, $N_s = 0, 1, 2, 5, 8, 10$.

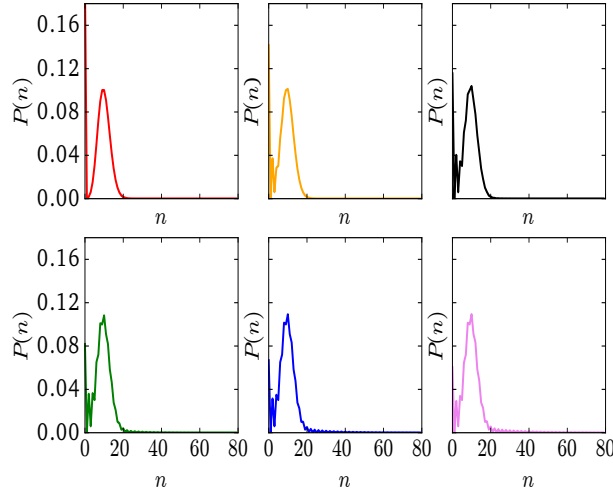


FIG. 8: $P(n)$ vs n for MSCS for $N_c = 10$, $N_s = 0, 1, 2, 5, 8, 10$ and $q = 0.8$.

We have plotted the atomic inversion in Figs. 9 and 10. As earlier here also $W(t)$ starts from the atomic dynamics of a coherent state for PSCS but for MSCS it starts from a oscillatory pattern, because this time the initial state is a MSCS, a mixture of coherent state and squeezed vacuum state. Now, if we begin to increase the value of N_s , $W(t)$ for MSCS gradually develops a pattern with decreasing amplitude in the collapse part of the dynamics. Its pattern tends towards that of a coherent state to some extent. But, for PSCS, $W(t)$ shows exactly the opposite behaviour. It starts from the dynam-

ics of a coherent state, but, with increasing value of N_s its pattern begins to get noisy with the larger amplitude of oscillations in the collapse part of the dynamics. We also observe that the duration of collapse time begins to decrease with increasing N_s and ultimately goes away with replaced ringing-revivals pattern.

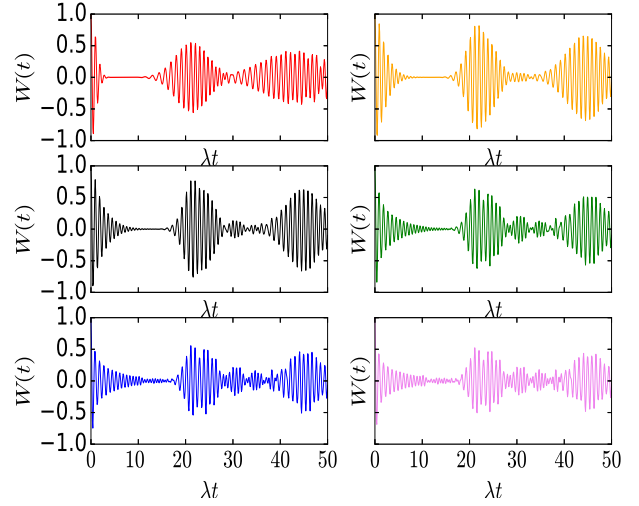


FIG. 9: Atomic inversion $W(t)$ vs λt for PSCS for $N_c = 10$, $N_s = 0, 1, 2, 5, 8, 10$.

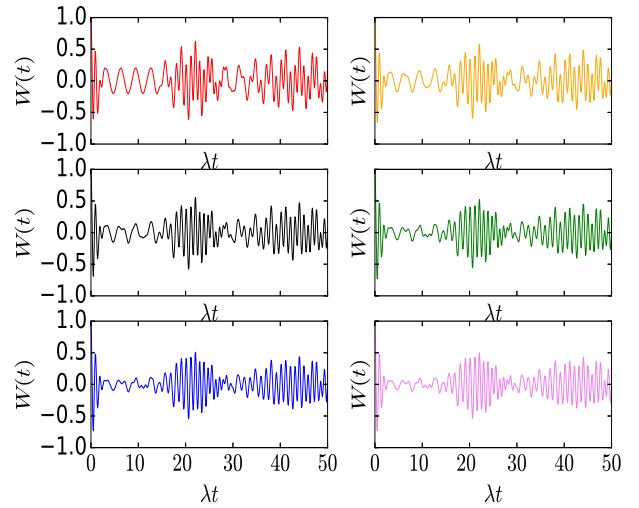


FIG. 10: Atomic inversion $W(t)$ vs λt for MSCS for $N_c = 10$, $N_s = 0, 1, 2, 5, 8, 10$, $q = 0.8$.

C. Entanglement dynamics

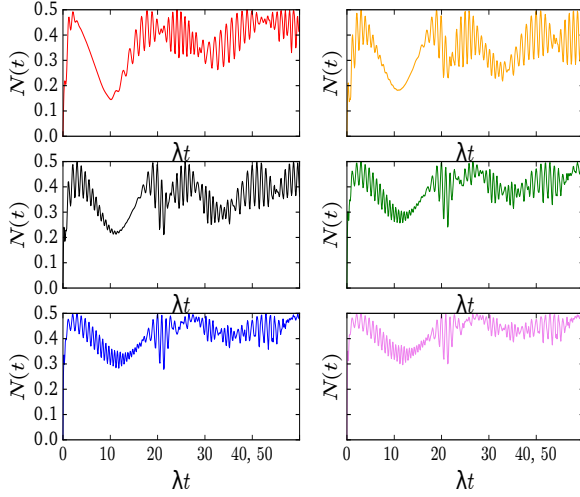


FIG. 11: Entanglement dynamics $N(t)$ vs λt for PSCS for $N_c = 10$, $N_s = 0, 1, 2, 5, 8, 10$.

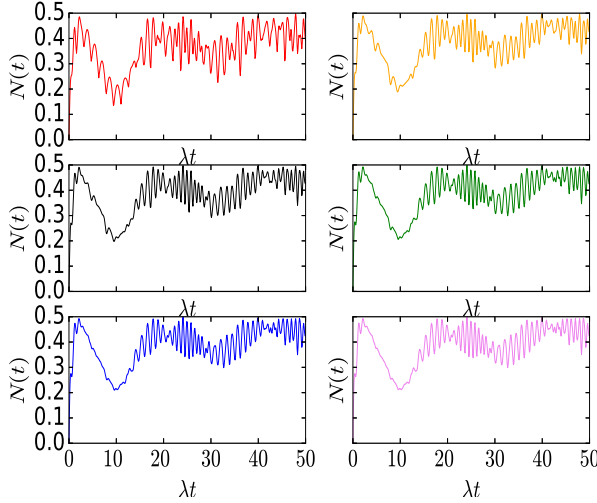


FIG. 12: Entanglement dynamics $N(t)$ vs λt for MSCS for $N_c = 10$, $N_s = 0, 1, 2, 5, 8, 10$, $q = 0.8$.

The temporal evolution of $N(t)$ vs λt is shown in Figs. 11 and 12. Here we see that $N(t)$ shows the coherent state dynamics for the PSCS, but, for the MSCS, its behaviour is very noisy. Now, as we increase the squeezing N_s , $N(t)$ behaves very differently. From the curves of the corresponding plots we see that, for PSCS, $N(t)$ begins to deviate from the coherent state dynamics and tends to a noisy behaviour. Interestingly, for MSCS, it behaves exactly in the opposite way. Here, $N(t)$ begins from a very noisy pattern and tends to the pattern of a coherent state dynamics. It tends more rapidly to the coherent dynamics than the atomic inversion. It is very non-intuitive that it tends towards the classical state pattern due to the addition of quantum noise.

VII. QUADRATURES SQUEEZING

The next quantity we want to investigate is the quadrature squeezing for fixed q . The two conjugate quadratures for the radiation field are defined as [16]

$$\hat{X}_1 = \frac{1}{2}(\hat{a} + \hat{a}^\dagger), \quad (34)$$

$$\hat{X}_2 = \frac{1}{2i}(\hat{a} - \hat{a}^\dagger). \quad (35)$$

The expectation values of these two quadratures for MSCS are

$$\langle \hat{X}_1(t) \rangle = q|\alpha| \cos(\omega t - \phi), \quad (36)$$

$$\langle \hat{X}_2(t) \rangle = -q|\alpha| \sin(\omega t - \phi), \quad (37)$$

where $\alpha = |\alpha| \exp(i\phi)$.

Now, the variances of these quadratures are given by

$$(\Delta \hat{X}_1)^2 = \frac{q}{4} + \frac{1-q}{4} [\cosh^2 |\zeta| + \sinh^2 |\zeta| - 2 \cosh |\zeta| \sinh |\zeta| \cos(2\omega t - \theta)], \quad (38)$$

$$(\Delta \hat{X}_2)^2 = \frac{q}{4} + \frac{1-q}{4} [\cosh^2 |\zeta| + \sinh^2 |\zeta| + 2 \cosh |\zeta| \sinh |\zeta| \cos(2\omega t - \theta)]. \quad (39)$$

For $\theta = 0$ and $t = 0$, these variances become

$$(\Delta \hat{X}_1)^2 = \frac{q}{4} + \frac{1-q}{4} \exp(-2|\zeta|) < \frac{1}{4}, \quad (40)$$

$$(\Delta \hat{X}_2)^2 = \frac{q}{4} + \frac{1-q}{4} \exp(2|\zeta|) > \frac{1}{4}. \quad (41)$$

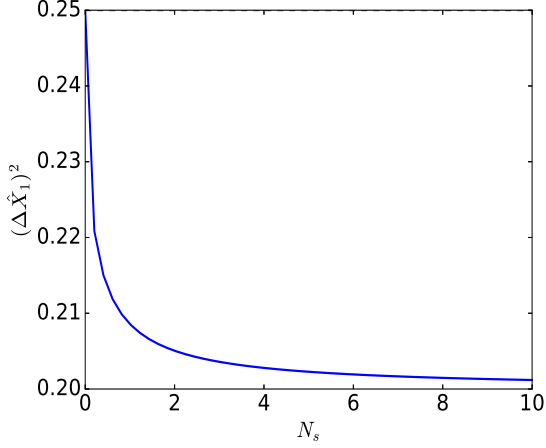


FIG. 13: Variance of quadratures $(\Delta \hat{X}_1)^2$ vs N_s for MSCS for $q = 0.8, N_c = 10$.

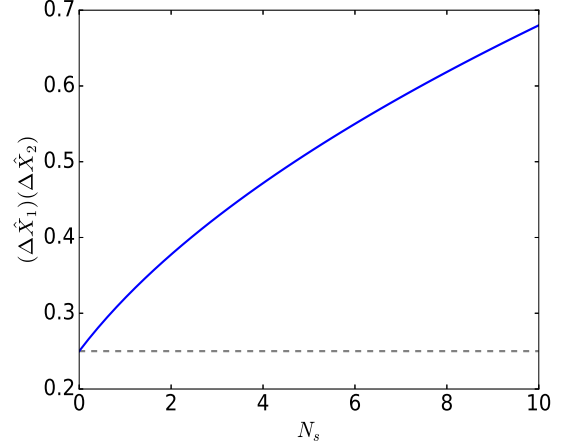


FIG. 15: $(\Delta \hat{X}_1)(\Delta \hat{X}_2)$ for MSCS for $q = 0.8, N_c = 10$.

. So, we see that MSCS is squeezed for nonzero r and $q \neq 1$. If, $N_s = 0$ i.e, $r = 0$, the uncertainties become minimum because MSCS is now a mixture of a coherent state and a vacuum state. The plots of the variances vs the squeezed photons are shown in Figs. 13, 14 and 15.

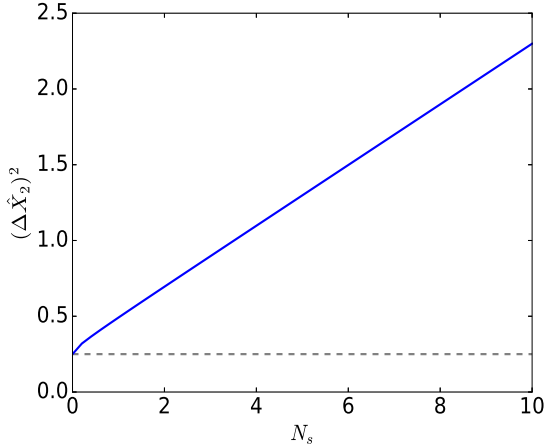


FIG. 14: Variance of quadratures $(\Delta \hat{X}_2)^2$ vs N_s for MSCS for $q = 0.8, N_c = 10, q = 0.8$.

VIII. MANDEL'S Q PARAMETER

Mandel's Q parameter is defined by [19]

$$Q = \frac{\langle (\Delta n)^2 \rangle}{\langle n \rangle} - 1, \quad (42)$$

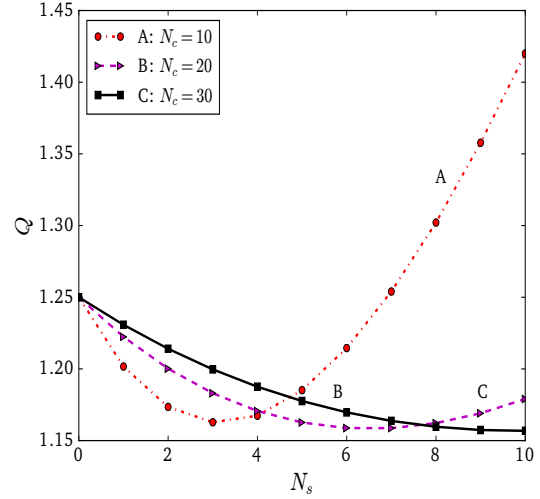


FIG. 16: Mandel's Q parameter vs N_s for MSCS for $N_c = 10, 20, 30$ and $q = 0.8$.

where $\langle n \rangle$ is the average number of photons. The plot of variation of Q with respect to N_s for MSCS is shown in Fig. 16. We observe that Q is always greater than zero. So, we conclude that MSCS shows super-Poissonian statistics. The variation in Q is maximum for $N_c = 10$ and minimum for $N_c = 30$. For PSCS, Q parameter has been calculated by Subeesh *et al.* [3]. They observed that PSCS shows sub-Poissonian statistics around a particular value of N_s for a specific value of N_c . This value of N_s causes the localization in PCD for PSCS. But, for large values of N_s it shows super-Poissonian statistics.

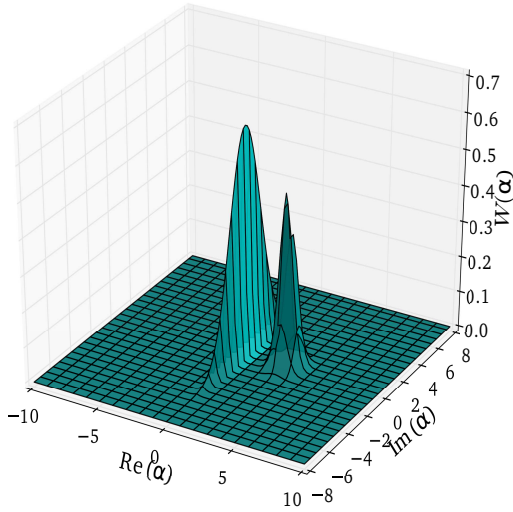


FIG. 17: Wigner function for MSCS for $N_c = 10$, $N_s = 2$ and $q = 0.8$.

IX. WIGNER FUNCTION

The Wigner function $W(\alpha)$ is well known in literature and it is defined as [19]

$$W(\alpha) = \frac{1}{\pi^2} \int d^2\beta \text{Tr}[\hat{\rho}\hat{D}(\beta)] \exp(\beta^*\alpha - \beta\alpha^*). \quad (43)$$

The density operator for MSCS is given by

$$\hat{\rho}_{\text{mixed}} = q|\alpha\rangle\langle\alpha| + (1-q)|\zeta\rangle\langle\zeta|. \quad (44)$$

So, $W(\alpha)$ for this state is given by

$$W(\alpha) = q\frac{2}{\pi} \exp(-2|\alpha - \gamma|^2) + (1-q)\frac{2}{\pi} \exp(-|\alpha \cosh|\zeta| - \alpha^* e^{i\phi} \sinh|\zeta||^2) \quad (45)$$

Fig. 17 depicts $W(\alpha)$ for MSCS. We see that $W(\alpha)$ is a combination of two Gaussians at two different positions in phase space and it is positive at all points. The Wigner functions for both PSCS and MSCS are positive.

X. CONCLUSION

We see from the observations that various properties and the dynamics of atom-field interaction for PSCS and MSCS are very different and contrasting. The addition of the squeezed photons to the coherent photons has very different effects on the atomic inversion and entanglement dynamics for PSCS and MSCS. In the case of variable q , both the dynamics $W(t)$ and $N(t)$ starts from the dynamics of a coherent state field. But, with the addition of increasing value of squeezed photons atomic-field dynamics for

both the fields show oscillatory behaviour. We observe that for MSCS, the dynamics is more sensitive to squeezed photons as compared to that of PSCS.

In the case of fixed value of q , for PSCS, both the dynamics i.e., the atomic inversion and the entanglement dynamics start from the pattern of a coherent state. On increasing the squeezed photons, the patterns gradually become noisy. Interestingly, for MSCS, it is quite the opposite. In this case, the atomic inversion and the entanglement dynamics start from a very noisy behaviour, but it tends towards that of a coherent state with increasing squeezed photons.

ACKNOWLEDGMENTS

We thank Dr. S. Sivakumar and Mr. Sushant Sharma for the discussions and suggestions.

-
- [1] Jaynes, E. T. & Cummings, F. W. *Proceedings of the IEEE* **51**, 89–109 (1963). URL <https://doi.org/10.1109/PROC.1963.1664>.
 [2] Barnett, S. & Radmore, P. M. *Methods in theoretical quantum optics*, vol. 15 (Oxford University Press,

- 2002).
 [3] Subeesh, T., Sudhir, V., Ahmed, A. & Satyanarayana, M. V. *Nonlinear Optics and Quantum Optics* **44**, 235 (2012). URL <https://arxiv.org/abs/1203.4792>.

- [4] Satyanarayana, M. V., Vijayakumar, M. & Alsing, P. *Physical Review A* **45**, 5301 (1992). URL <https://link.aps.org/doi/10.1103/PhysRevA.45.5301>.
- [5] Sivakumar, S. *The European Physical Journal D* **66**, 1–7 (2012). URL <https://doi.org/10.1140/epjd/e2012-30399-2>.
- [6] Mouloudakis, G. & Lambropoulos, P. **8**, 72 (2021). URL <https://doi.org/10.3390/photonics8030072>.
- [7] Hu, L.-Y. & Zhang, Z.-M. *JOSA B* **30**, 518–529 (2013). URL <https://doi.org/10.1364/JOSAB.30.000518>.
- [8] Israel, Y. *et al. Optica* **6**, 753–757 (2019). URL <https://doi.org/10.1364/OPTICA.6.000753>.
- [9] A. Büyükaşık, Ş. & Çayır, Z. *Journal of Mathematical Physics* **60**, 062104 (2019). URL <https://doi.org/10.1063/1.5050489>.
- [10] Podoshvedov, S. A. *Physical Review A* **87**, 012307 (2013). URL <https://link.aps.org/doi/10.1103/PhysRevA.87.012307>.
- [11] Podoshvedov, S. A. *Optics Communications* **290**, 192–201 (2013). URL <https://doi.org/10.1016/j.optcom.2012.09.018>.
- [12] Loudon, R. & Knight, P. L. *Journal of modern optics* **34**, 709–759 (1987). URL <https://doi.org/10.1080/09500348714550721>.
- [13] Yuen, H. P. *Physical Review A* **13**, 2226 (1976). URL <https://doi.org/10.1103/PhysRevA.13.2226>.
- [14] Jethwani, P. *M.Sc Dissertation (unpublished)*, Department of Physics, Indian Institute of Technology Madras, India (2017).
- [15] Satyanarayana, M. V., Rice, P., Vyas, R. & Carmichael, H. *Journal of Optical Society of America B* **6**, 228–237 (1989). URL <https://doi.org/10.1364/JOSAB.6.000228>.
- [16] Gerry, C., Knight, P. & Knight, P. L. *Introductory quantum optics* (Cambridge university press, 2005).
- [17] Wei, T.-C. *et al. Physical Review A* **67**, 022110 (2003). URL <https://link.aps.org/doi/10.1103/PhysRevA.67.022110>.
- [18] Nielsen, M. A. & Chuang, I. *Quantum computation and quantum information* (Cambridge University Press, 2010).
- [19] Agarwal, G. S. *Quantum optics* (Cambridge University Press, 2012).